Progress In Electromagnetics Research, PIER 74, 85–112, 2007

STUDY ON SHIELDING EFFECTIVENESS OF METALLIC CAVITIES WITH APERTURES BY COMBINING PARALLEL FDTD METHOD WITH WINDOWING TECHNIQUE

J. Z. Lei, C. H. Liang, and Y. Zhang

National Key Laboratory of Antennas and Microwave Technology
Xidian University
Xi'an 710071, Shaanxi, P. R. China

Abstract—A novel hybrid method combining 3D Parallel Finite-Difference Time-Domain (FDTD) method with Windowing technique through a new Controlling factor to study the Shielding Effectiveness (SE) of metallic cavities with apertures is firstly presented in this paper. The simulating time when the sampling electric field in cavity converges can be reduced greatly by the MPI-based Parallel FDTD method with the optimum virtual topology for the scattering problem. And then the sampling electric field in cavity is dealt with Windowing technique, which can further reduce the total time steps that Parallel FDTD method needs. The numerical results show that combination of Parallel FDTD with Windowing technique can enhance the simulating efficiency greatly. Finally, the SE of metallic cavities with different configurations is studied by the hybrid method and some useful conclusions to the practical electromagnetic shielding problems are obtained.

1. INTRODUCTION

Coupling of high power electromagnetic pulse into cavities through apertures is an important issue in EMC and EMI. Electronic equipment used in communication is usually shielded in order to increase reliability and integrity. In addition, electronic equipment is commonly housed into metallic boxes, but the apertures that serve ventilation on them compromise the integrity. In such structures, the external electromagnetic fields can directly couple energy into the interior through apertures. Sometimes the energy may interfere with or destroy the electronic system. Therefore, the shielding effectiveness (SE) of

cavities with apertures is a crucial issue and should be taken into account during design and manufacture of the electronic systems.

The SE of cavities with apertures has been studied with different methods [1–6] recently. Mendez [1] analytically formulated the SE of a cavity with electrically small apertures using dual Green Function and minipore scattering theory. In [2] a technique to analyze the SE of a cavity with electrically large apertures was presented according to energy conservation law. Furthermore, the method of equivalent transmission line was successfully used in [3] for the SE analysis. In [4] field distributions of cavities with apertures were given by the FDTD method with the incidence of EM pulse. Additionally, in [5] FDTD was also employed to sinusoidal steady-state penetration problems and the corresponding SE was obtained.

FDTD is a powerful numerical technique, which is currently used for the analysis of a wide variety of EM field problems such as radiation and scattering of EM field, microwave and millimeter wave circuits and EMC etc where it has achieved greatly successful applications. On the other hand, FDTD requires large amounts of computer memory and long simulation time, which becomes the limiting factor when it is used to solve EM field problems of objects with resonance characteristic or electrically large size such as cavities with electrically small apertures.

Parallel FDTD method is an effective way to solve the issues. This paper adopts MPI-based Parallel FDTD to analyze the SE of cavities with apertures efficiently. Besides, Windowing technique is also employed to quicken the simulation. Using Windowing technique to deal with the sampling electric field in time domain can reduce the total time steps that Parallel FDTD method needs. To exert their advantages respectively, a novel hybrid method combining Parallel FDTD with Windowing technique through a new Controlling factor is firstly proposed in this paper.

In Section 2, we mainly define the new Controlling factor and present how to hybrid the two methods. In Section 3, the optimum virtual topology of Parallel FDTD for the scattering problem is firstly obtained through an in-depth study. The SE of a cavity with a rectangular aperture is computed by the hybrid method. The results obtained validate it right and efficient. In Section 4, the SE of several kinds of cavities with apertures is analyzed by the hybrid method and some useful conclusions are obtained which can assist the design of electronic systems.

2. BASIC THEORY

2.1. Definition of Shielding Effectiveness

SE (Shielding Effectiveness) is used to value the effect of shielding in electromagnetic coupling problems of cavities with apertures. The definition of SE is based on a plane wave excitation and the following procedure.

(1) Excite the cavity with an incident pulse plane wave and record the electric field at the position of interest.

(2) Excite an empty space computational domain with the same incident pulse plane wave and record the electric field at the position of interest.

(3) Fourier transform the time-domain data.

(4) Compute the SE in decibels using the following definition:

$$SE = 20 \log \left(\frac{\text{empty space frequency response } E_1}{\text{problem space frequency response } E_2} \right) \quad (1)$$

2.2. Parallel FDTD Algorithm

In general, Parallel FDTD [6] computation is what subdivides the whole FDTD computation space into several sub-domains. Each process calculates field values in one or more sub-domains. The iterative solution of FDTD is able to continue by transferring field values across the interfaces between the neighboring processes. In short, there are three patterns to subdivide the whole space into sub-domains in Parallel FDTD, which results in three data communication patterns: 1D, 2D and 3D communication pattern of Parallel FDTD. This paper adopts 3D communication pattern, which is introduced in the following.

As shown in Fig. 1(a), the computation space is subdivided into nearly equal parts in the three directions. The virtual topology of the processes' distribution is chosen in a similar shape to the problem partition. Each sub-domain is mapped to its associated node where all the field values belonging to this sub-domain are computed. To update field values lying on interfaces between sub-domains, it is necessary to transfer data between neighboring processes. A X-Z slice of the computation space at one of the interfaces between nodes in the y-direction is shown in Fig. 1(b).

The parallel code of this work is written in Fortran 90 format and run on a PC cluster that belongs to National Key Laboratory of Microwave and Antennas Technology in China. The parameters of the Cluster are listed below:

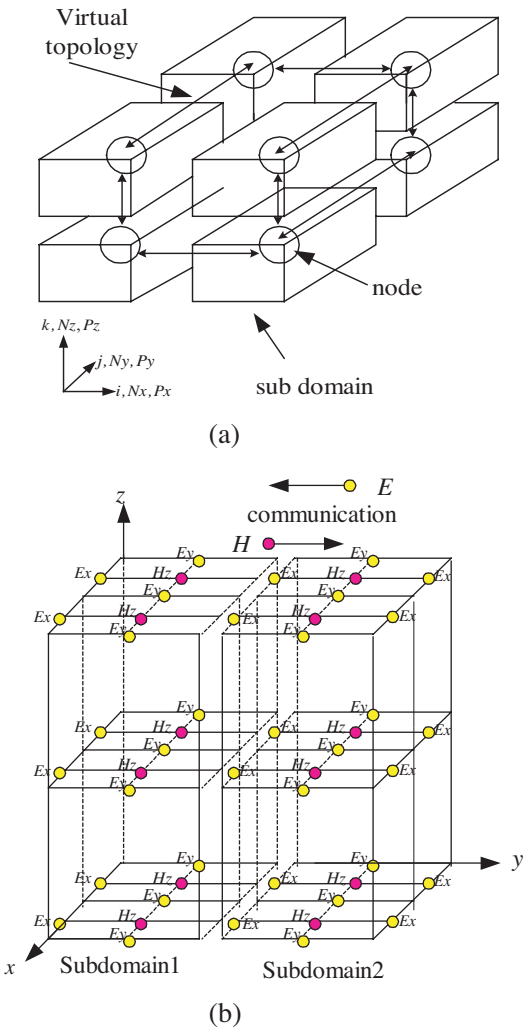

Figure 1. Division and communication of Parallel FDTD in 3D. (a) partition of the simulated problem (b) field components communication.

10-Node.
Pentium IV 2.8C GHz CPU per Node
1.0 GBytes Memory per Node
1000 M High-speed Network Interface Card
1000 M Bites Switch

The photo of the PC cluster is shown in Fig. 2

Figure 2. Photo of the PC cluster.

2.3. Windowing Technique

In electromagnetic analysis, various quantities which describe different characteristics of a problem such as gain, input impedance, RCS, SE, etc., are often defined in the frequency domain. Therefore, a transformation must be used to convert the quantities computed by time-domain methods (like the FDTD) into the frequency domain. This transmission is usually performed using a Fourier process (FFT or DFT). Theoretically, the DFT summation has to be infinite. However the DFT summation will be of finite extent in practice, which introduces errors in the computation. For this reason, FDTD simulations usually have to allow sufficient time without introducing large errors. But in some SE computations of high-quality factor structures, tens or even hundreds of thousands of time-steps may be required for the sampling fields to converge. Windowing is an useful technique to overcome the problem. Windows are weighting functions that multiply the signal of interest. Windowing can shorten the simulation time through truncating the sampling field correctly.

Let the signal of interest be $f(t)$ and the window $w(t)$. Then, the windowed signal, $f_w(t)$, can be written as

$$f_w(t) = f(t)w(t) \tag{2}$$

From basic theory of signals and systems, it is well known that the FT of the windowed signal, is the convolution of the FTs of $f(t)$ and $w(t)$

$$F_w(\omega) = F(\omega) * W(\omega) \tag{3}$$

It needs to be pointed out that types of windows have been used in signal processing, such as Hanning, Blackman-Harris, Kaizer,

Hamming, etc. Hanning window is employed as the window function in this paper. Assuming that the window centers the zero time and adopts $(N + 1)$ sampling points, that is $w(n), n = -N/2, \ldots, 0, \ldots, N/2$, Hanning window can be written as

$$w(n) = \cos^2\left(\frac{\pi n}{N}\right) \tag{4}$$

2.4. Mechanism of the Novel Hybrid Method

As we know, windowing the time-domain quantity that Parallel FDTD outputs can reduce the time steps FDTD needs. However, it is still a problem at which time step the time-domain data should be windowed. Previous literatures [7] give the time step windowed directly according to experience and estimation, which is not convictive obviously. A new automatic mechanism which can choose a proper time step to execute the Windowing is firstly presented in this paper.

2.4.1. Definition of Controlling Factor

We have a point of view that the computed SE curve will drive to coincident as the time steps increase and almost has no difference when the time steps become long to a special extent. Based on this standpoint, Controlling factor is proposed to determine the time step when the time-domain data is windowed.

To define the Controlling factor, Controlling function S_i must be defined firstly. Controlling function reflects the difference of two SE curves which have the same time interval and the same number of frequency sampling points. Controlling function S_i is based on the following procedure.

(1) Window the time-domain data and compute the SE with n frequency sampling points when the time steps are $T_{i-1}(i \geq 1)$.

(2) Window the time-domain data and compute the SE with n frequency sampling points when the time steps are $T_i(T_i - T_{i-1} = \Delta t$, Δt= constant)

(3) Compute the Controlling function using the following definition:

$$S_i = \sum_{f_i=f_1}^{f_n} |SE_i(f_i) - SE_{i-1}(f_i)| \tag{5}$$

Having the definition of S_i, we can define Controlling factor as a number that approximates to the minimum value of S_i. The amplitude of the Controlling factor can control the accuracy degree of SE curves.

Obviously, S_i will be close to zero if the time steps are infinite. The smaller the amplitude of S_i is, the more accurate the computed SE is.

2.4.2. The Flow Process Chart of the Mechanism

In this paper, we windowed the time-domain data from 5000 time steps and the time interval is also 5000 time steps, which need a very short simulation time for Parallel FDTD. The SE curves are obtained at 5000 time step, 10000 time step, 15000 time step and etc. The SE curves are marked with SE_1, SE_2, $SE_3, \ldots SE_n$. Then according to the definition of S_i, we compute a series of S_i. When $S_i \leq Controlling$ factor, the program ends and the SE at this time step is deemed to be correct. The flow process chart of the novel mechanism is shown in Fig. 3.

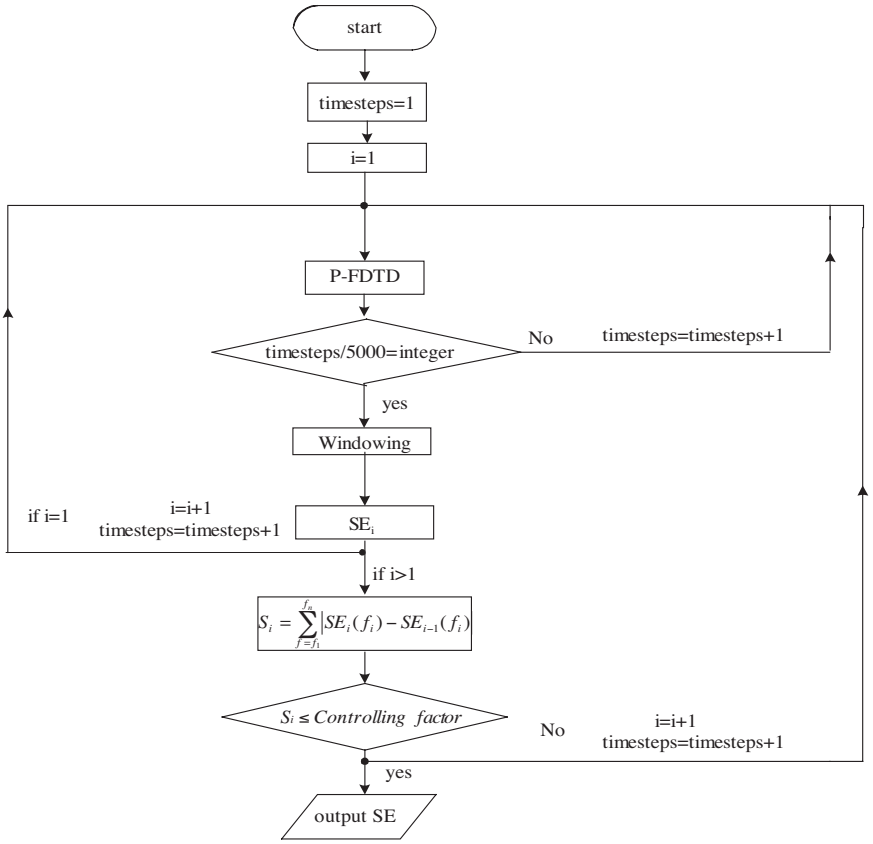

Figure 3. The flow process chart of the novel method.

3. EXAMPLES FOR VALIDATION

3.1. Physical Model

In this section, the SE of two different geometries is examined. Consider a $30 \times 12 \times 30$-cm rectangular metallic cavity as shown in Fig. 4. For the case (see Fig. 4(a)), this paper uses Parallel FDTD to compute the SE. Also the optimum virtual topology for the scattering problem is obtained though that for the radiating problem has been solved in [6]. And then this paper analyzes the SE of the cavity with a rectangular aperture (see Fig. 4(b)) by the hybrid method. Here, all the analysis presented involves SE computations of both two geometries

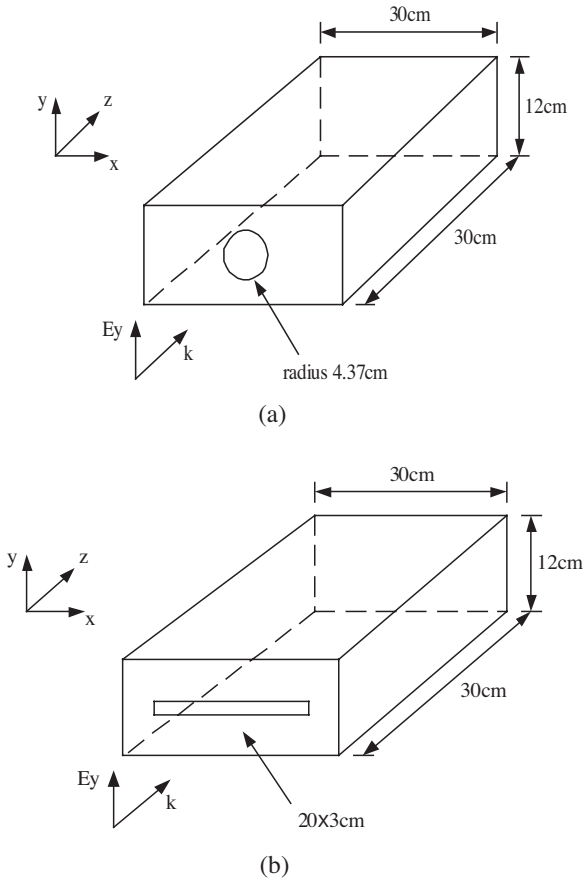

Figure 4. Two geometries for validation. (a) 1#Cavity with a circular aperture. (b) 2#Cavity with a rectangular aperture.

at the center of the metallic cavity. Ten UPML is employed and the exciting plane is placed 10 grids away from the UPML Total-scatter field plane in order to avoid undesired effects during the computation. The incident plane wave is Gauss wave

$$E_{inc}(t) = E_0 \times e^{-9(t-t_0)^2/\tau^2} \tag{6}$$

In this formula, $E_0 = 1.0 \times 10^3$ v/m and $t_0 = \tau = 2.5 \times 10^{-10}$ s.

3.2. Analyzing the Cavity with the Circular Aperture

In this case, the Parallel FDTD method is employed to simulate the cavity with the circular aperture (Fig. 4(b)). The increment $dx = dy = dz = 0.3$ cm is used here and the amount of the FDTD grids is $180 \times 90 \times 140$.

Figure 5 presents the SE of the geometry obtained by Parallel FDTD, which agrees well with the measurement and the results obtained by using MLFMM and transmission-line model method. Simulating this structure with resonance characteristic, 250,000 time steps are required to achieve the stable total electric field involved. 9.7 hours is required with eight PC Nodes and about 72.8 hours with a single PC Node of the PC Cluster. So the parallel technique can save the simulation time greatly, which proves the Parallel FDTD method right and efficient.

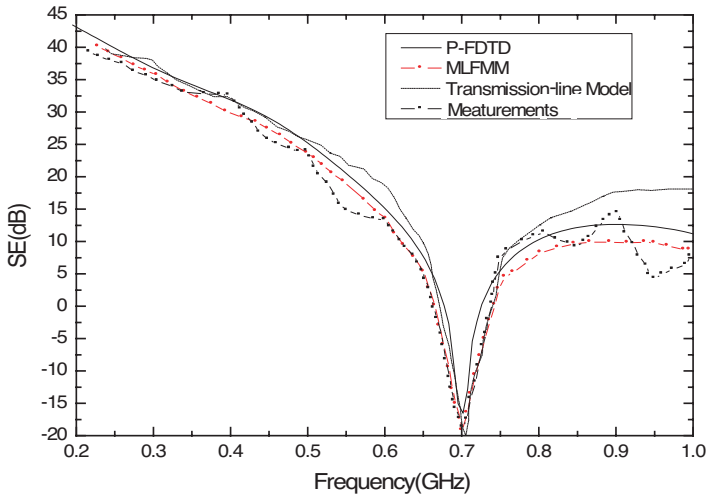

Figure 5. Comparison with different methods(1#cavity).

In the following, we analyze the performance of Parallel FDTD method for the problem.

Table 1 is the comparison of total computation time (in seconds) with different PC Nodes and different virtual topology schemes in 1000 time-steps.

Table 1. Comparison of computation time.

Title	PC Nodes	Virtual topology ($x \times y \times z$)	Computation time(sec)
FDTD	1	1×1×1	4221.18
P-FDTD	2	1×2×1	2191.81
P-FDTD	2	1×1×2	2160.59
P-FDTD	2	2×1×1	2125.99
P-FDTD	4	1×1×4	1170.47
P-FDTD	4	4×1×1	1162.69
P-FDTD	4	1×2×2	1131.01
P-FDTD	4	2×2×1	1099.46
P-FDTD	4	2×1×2	1097.48
P-FDTD	5	1×5×1	1102.98
P-FDTD	5	1×1×5	997.12
P-FDTD	5	5×1×1	964.95
P-FDTD	6	6×1×1	869.24
P-FDTD	6	1×3×2	786.01
P-FDTD	6	2×3×1	781.51
P-FDTD	6	3×2×1	765.09
P-FDTD	8	1×2×4	611.00
P-FDTD	8	2×1×4	604.64
P-FDTD	8	4×2×1	604.40
P-FDTD	8	4×1×2	598.82
P-FDTD	8	2×2×2	575.25

Firstly, we will discuss the parallel performance of the Parallel FDTD using the different dimensional virtual topology with the same number of PC Nodes. In this case, the difference between the computing time is calculated with the shortest time as the reference.

CASE1: Four PC Nodes

The reference calculating time is 1097.48 seconds using the $2\times1\times2$ virtual topology scheme:

$$\begin{aligned}
\text{Comparison:}\quad & 1\times1\times4 \quad (1170.47-1097.48)=72.99\,(\text{sec})\\
& 4\times1\times1 \quad (1162.69-1097.48)=65.21\,(\text{sec})\\
& 1\times2\times2 \quad (1131.01-1097.48)=33.53\,(\text{sec})\\
& 2\times2\times1 \quad (1099.46-1097.48)=1.98\ (\text{sec})
\end{aligned}$$

CASE2: Eight PC Nodes

The reference calculating time is 575.25 seconds using the $2\times2\times2$ virtual topology scheme:

$$\begin{aligned}
\text{Comparison:}\quad & 1\times2\times4 \quad (611.00-575.25)=35.75\,(\text{sec})\\
& 2\times1\times4 \quad (604.64-575.25)=29.39\,(\text{sec})\\
& 4\times2\times1 \quad (604.40-575.25)=29.15\,(\text{sec})\\
& 4\times1\times2 \quad (598.82-575.25)=23.57\,(\text{sec})
\end{aligned}$$

From above, it is obvious that for the same number of PC Nodes, the more the dimension of the virtual topology is, the less the computation time is required. Note that in Table 1, 4 PC Nodes with proper virtual topology can bring us higher computational efficiency than 5 PC Nodes with improper virtual topology. That means properly choosing virtual topology is an approach to enhance efficiency besides increasing the PC Nodes.

Then we will discuss the computation efficiency of the same dimensional virtual topology (with the same number of PC Nodes) using the data in Table 1 in the following.

CASE 1: Four PC Nodes

The amount of the grids at interfaces in one dimensional virtual topology is compared as follows:

$$\begin{aligned}
& 1\times1\times4 \quad 180\times90\times(4-1)=48600\\
& 4\times1\times1 \quad (4-1)\times90\times140=37800
\end{aligned}$$

The amount of the grids at interfaces in two dimensional virtual topologies is compared as follows:

CASE 2: Eight PC Nodes

The amount of the grids at interfaces in two dimensional virtual topologies is compared as follows:

From above, it is obvious that the topology along the direction where the amount of the FDTD grids is larger can save the computation

$$
\begin{aligned}
&1 \times 2 \times 2 \quad 180 \times 140 + 180 \times 90 = 41400\\
&2 \times 2 \times 1 \quad 140 \times 180 + 140 \times 90 = 37800\\
&2 \times 1 \times 2 \quad 180 \times 90 + 140 \times 90 = 28800
\end{aligned}
$$

$$
\begin{aligned}
&1 \times 2 \times 4 \quad 140 \times 180 + (4-1) \times 180 \times 90 = 73800\\
&2 \times 1 \times 4 \quad 140 \times 90 + (4-1) \times 180 \times 90 = 61200\\
&4 \times 2 \times 1 \quad 140 \times 180 + (4-1) \times 140 \times 90 = 63000\\
&4 \times 1 \times 2 \quad 90 \times 180 + (4-1) \times 140 \times 90 = 54000
\end{aligned}
$$

time for the same dimensional virtual topology with the same number of PC Nodes, which is determined by the amount of the transferred data.

So we can obtain two conclusions which are the same as those in [6].

(1) If possible, the optimum virtual topology scheme should be created in three dimensions, and then the better is in two dimensions, which can bring us higher efficiency than in one dimension.

(2) As to the same dimensional virtual topology, the topology scheme should be created along the directions where the amount of the FDTD grids is larger.

The conclusions can adapt to not only the radiation but also the scattering of EM problems and it possesses the practical significance for the study of MPI-based Parallel-FDTD on PC clusters.

Based on these two conclusions, the following calculations all adopt the virtual topology scheme of $2 \times 2 \times 2$.

3.3. Analyzing the Cavity with the Rectangular Aperture

The Parallel FDTD method is firstly employed to simulate the cavity with the rectangular aperture and the increment $dx = dy = dz = 0.5\,\text{cm}$ is used here and the amount of the FDTD grids is $180 \times 90 \times 140$.

Simulating this structure with resonance characteristic, 250,000 time steps are required to achieve the stable total electric field involved. The time-domain FDTD response with the 250,000 time steps is shown in Fig. 6(a) and Fig. 6(b) shows the partial enlarged drawing.

This paper simulates the structure with 8 DELL computers with high performance and a single one, respectively. 9.43 hours is required with eight PC Nodes and about 74.37 hours with a single PC Node of the PC Cluster.

The SE curve of the geometry is shown Fig. 7. Again, the Parallel FDTD curve is in good agreement with the measured data, FEM and

FDTD results, which proves the efficiency and correctness of Parallel FDTD again.

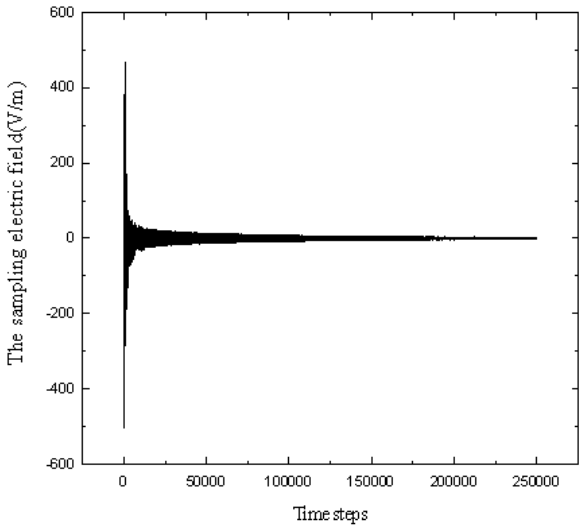

(a)

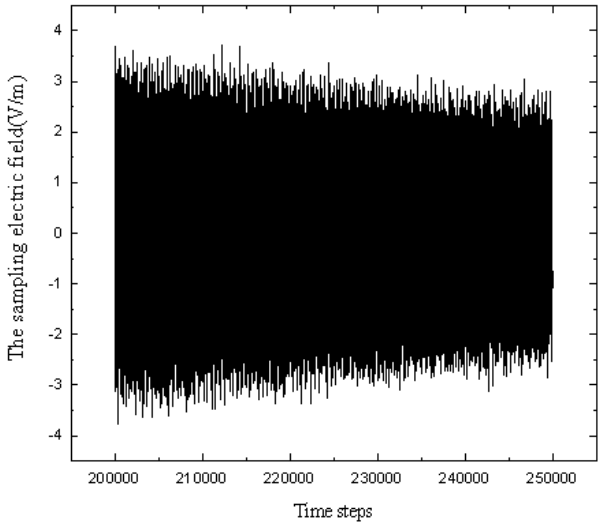

(b)

Figure 6. Time-domain FDTD response. (a) Time-domain response (b) partial enlarged drawing.

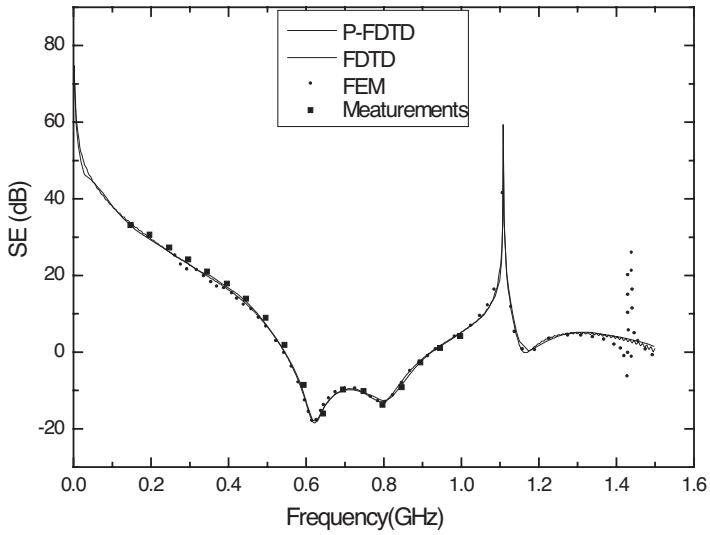

Figure 7. Comparison with different methods (2#cavity).

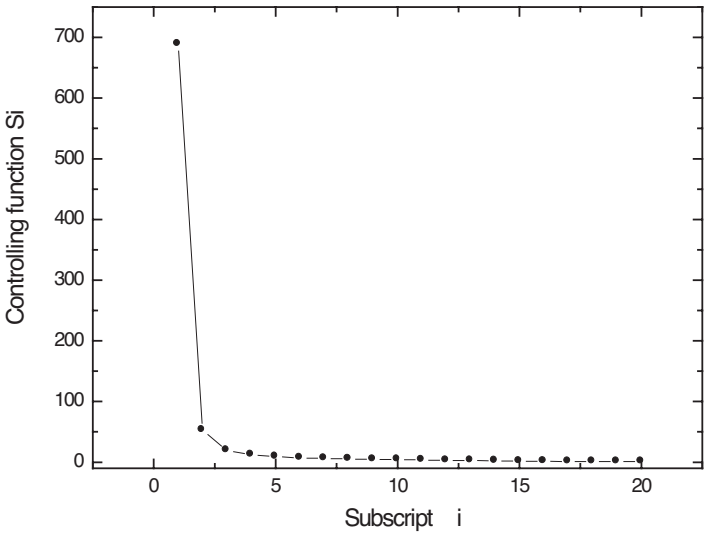

Figure 8. Curve of Controlling function S_i.

In the following, we analyze the structure using our hybrid method. Firstly, the Controlling factor is studied. Assuming that the time interval is 5000 time steps and the number of frequency sampling

points is 6606, we compute S_i from 10000 to 200000 time steps. The results are shown in Table 2 and Fig. 8 gives the S_i curve, which satisfies exponential distribution approximately. The actual result is in accordance with the theory above. It can be imaged that Controlling function will decay to zero if the time steps are infinite.

Table 2. Results of Controlling function S_i.

i	Time step of SE_i	Time step of SE_{i-1}	$S_i = \sum_{f=f_1}^{f_n} \lvert SE_i(f_i) - SE_{i-1}(f_i) \rvert$
1	10000	5000	689
2	20000	15000	52.9553
3	30000	25000	19.5478
4	40000	35000	12.1207
5	50000	45000	9.1288
6	60000	55000	7.2822
7	70000	65000	6.1163
8	80000	75000	5.2923
9	90000	85000	4.4738
10	100000	95000	4.4217
11	110000	105000	3.6034
12	120000	115000	2.9409
13	130000	125000	2.7206
14	140000	135000	2.2269
15	150000	145000	1.4972
16	160000	155000	1.4335
17	170000	165000	1.1847
18	180000	175000	1.1682
19	190000	185000	1.1324
20	200000	195000	1.1152

Next we should choose proper Controlling factor to obtain the correct SE. Note that Controlling factor is a variable parameter and it can be chosen according to the computation condition. The basic principle to choose Controlling factor is to make the obtained SE curve smooth. To make the result more accurate, the Controlling factor should be chosen as small as possible. Through an in-depth comparison study with the result in literatures, the SE when the time steps are

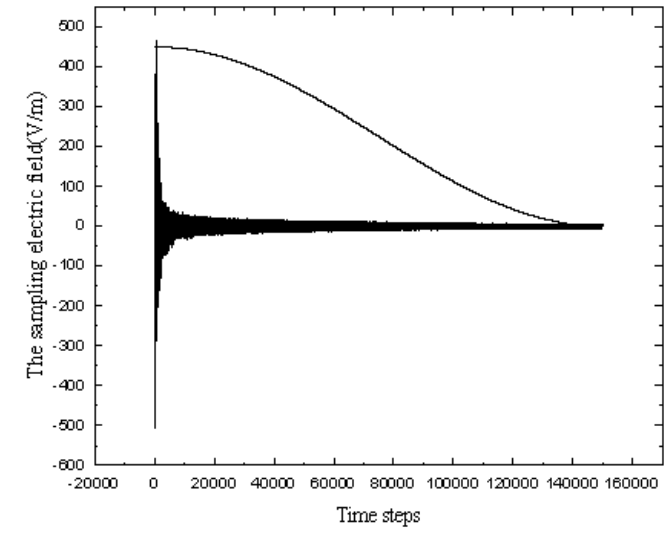

(a)

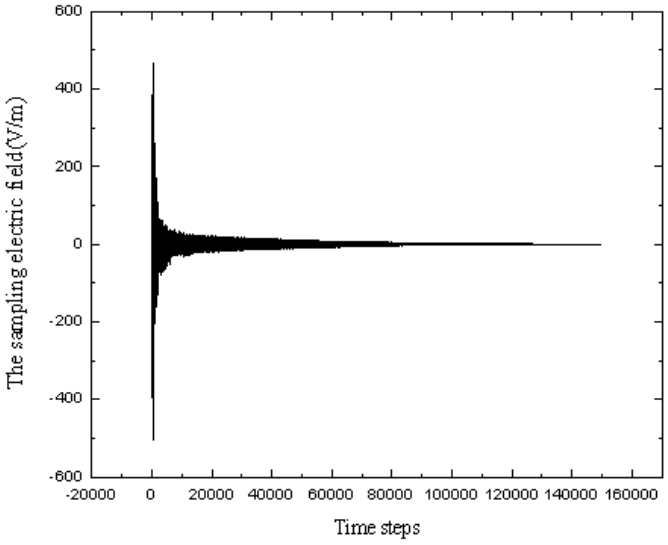

(b)

Figure 9. The Windowing process. (a) Time-domain data along with Hanning window (b) Windowed data.

150,000 can be thought to be correct. The windowed time-domain FDTD response is formed by multiplying the positive time half of the Hanning window with the first 150,001 time-domain points (see Fig. 9). It is easily seen that the field amplitude decays to zero more quickly than the initial data. The corresponding SE curve is illustrated in Fig. 10. The response curve using Windowing technique is smooth, which is in good agreement with the reference results. Upon that, we can choose the Controlling factor as 1.5. Note the factor is only applicable for 5000 time steps interval and 6606 sampling frequency points.

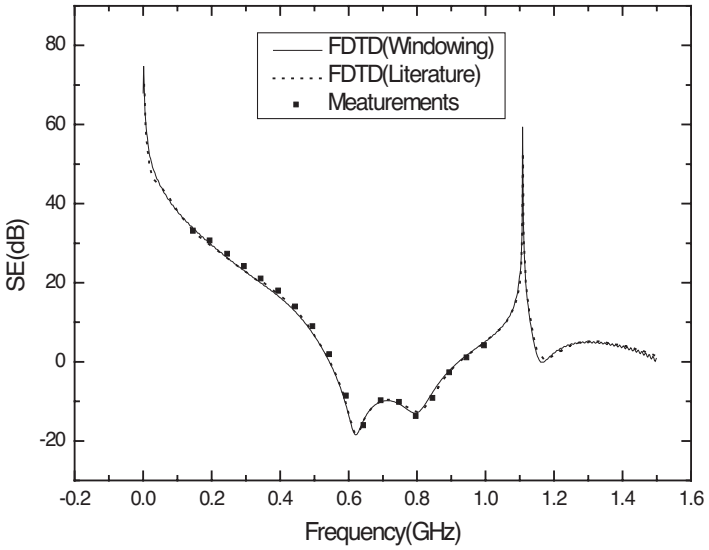

Figure 10. SE curve using Windowing technique.

Because the Controlling factor reflects the fitting degree of two curves, it can be used in other cases. Based on that, the SE analysis of the following geometries uses the Controlling factor of 1.5, too.

Figure 11 illustrates the SE computed by Parallel FDTD with Hanning window and without it at 150000 time steps. Obviously, there are significant oscillations in the response without Windowing. So using Windowing technique to truncate the time-domain data can reduce the simulating time greatly. Parallel FDTD simulations for 150,000 time-steps cost 4.65 hours while 36.28 hours using FDTD in a single computer.

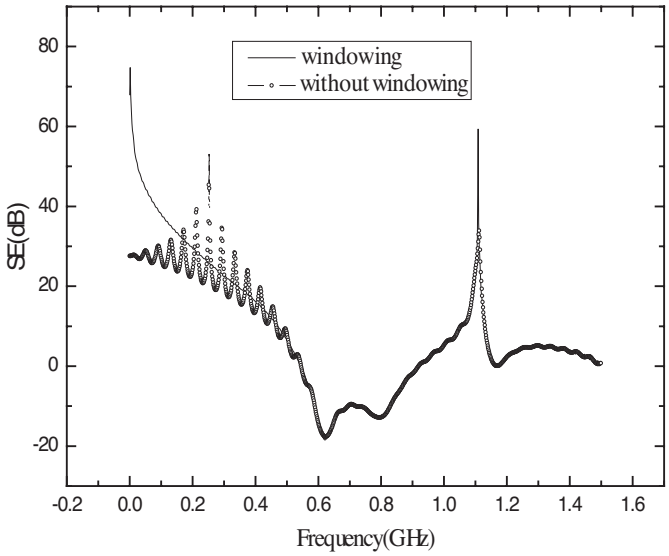

Figure 11. SE with Hanning window.

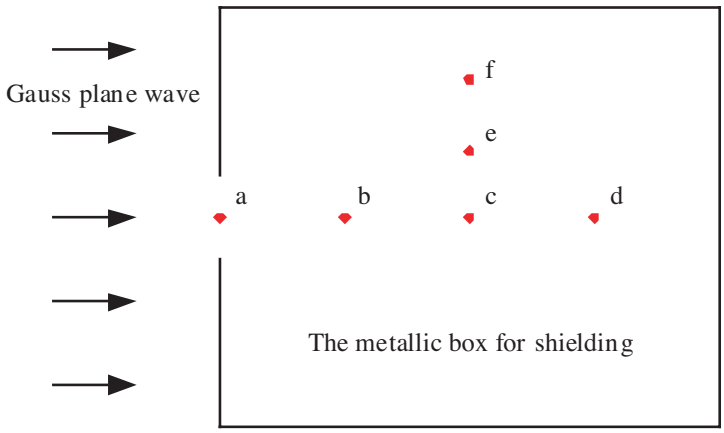

Figure 12. The points at different positions.

4. SEVERAL KINDS OF STRUCTURES

Having validated the novel hybrid method, we next proceed to examine the SE of other different geometries. The purpose of this study is to examine the role of various apertures on coupling behavior and assist the design of electronic systems.

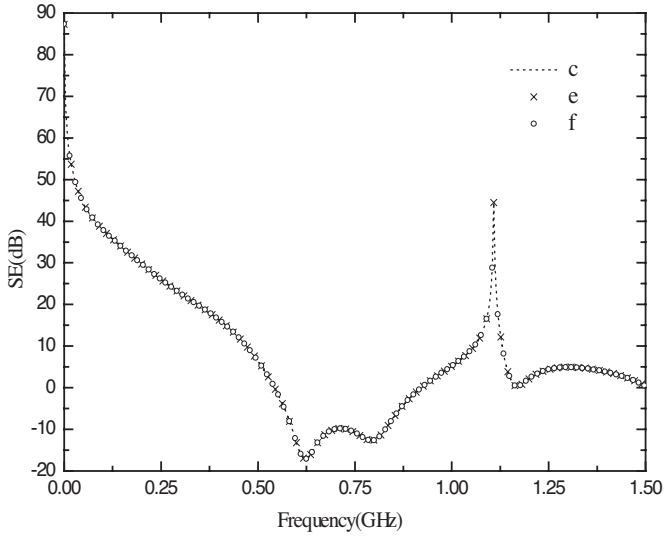

(a) SE of c, e and f

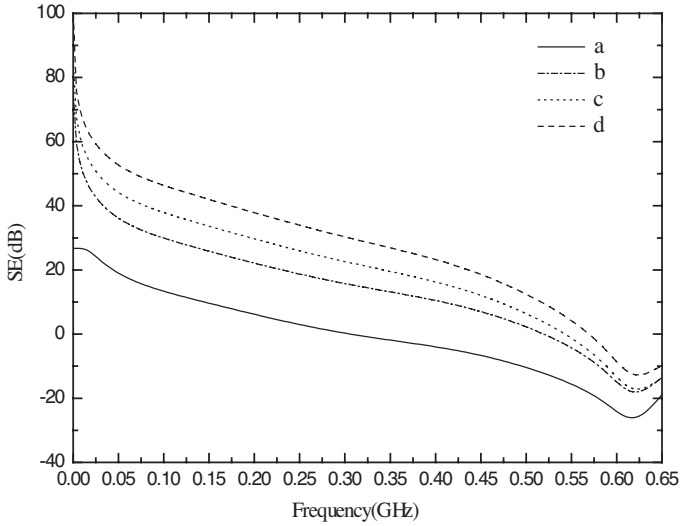

(b) SE of a, b, c and d

Figure 13. SE of different points. (a) SE of c, e and f (b) SE of a, b, c and d.

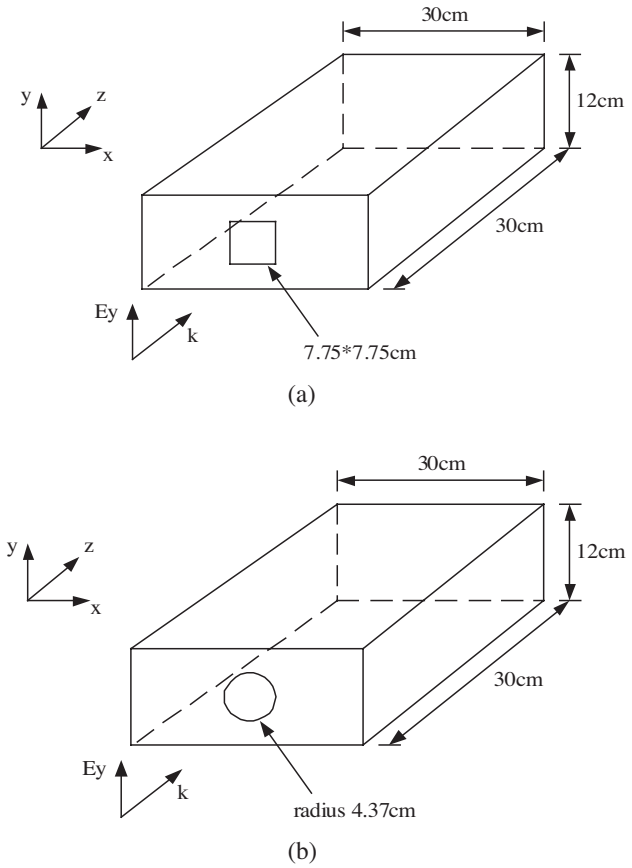

Figure 14. Apertures with different shapes. (a) The square aperture (b) The circular aperture.

4.1. The Position of Different Sampling Points

In the SE analysis of the same structure, different sampling points will have different SE. We still consider the same $30 \times 12 \times 30$-cm cavity (see Fig. 4(a)) with the 20×3-cm aperture. The SE of 6 different points is computed (Fig. 12). Fig. 13(a) plots the SE curves of c, e and f point. The SE curves of a, b, c, and d point are given in Fig. 13(b). The SE curves of c, e and f point are almost identical, so the points with the same distance away from the wall which the aperture is on have similar SE. From Fig. 13(b), it can be concluded that at lower frequencies the points which are farther away from aperture have the better SE and

the SE of b and c point is almost the same at 625 MHz. From this conclusion, IC circuit module should be installed as far away from the aperture in the design of electric system as possible.

4.2. Different Aperture Shapes

We next proceed to examine the SE of the cavity with a 7.75×7.75-cm-square aperture and a circular (4.37-radius) aperture(see Fig. 14) with the same area as a 20×3-cm rectangular aperture (see Fig. 4(a)). To ensure the accuracy, MLC-FDTD [6] is used for the circular aperture. SE curves are given in Fig. 15. The structures of the circular and square apertures of the same area are seen to have the similar SE. However the SE of circular and square apertures is much higher at lower frequencies than the rectangular aperture of the same area. This is due to the shifting of the aperture resonance to higher frequencies and away from the original aperture resonance at 625 MHz.

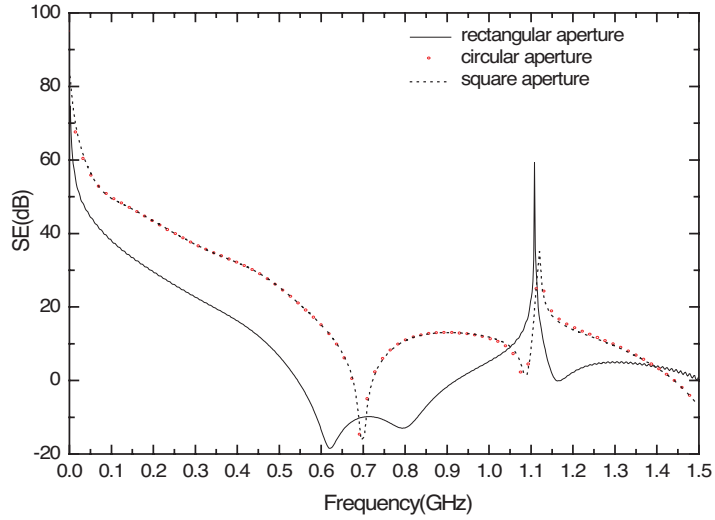

Figure 15. SE of the apertures with different shapes.

Through the analysis above, we should use square and circular apertures instead of the rectangular aperture when apertures have to be used in shielding boxes. Square or circular apertures can be chosen freely according to practical situation because of the similar SE.

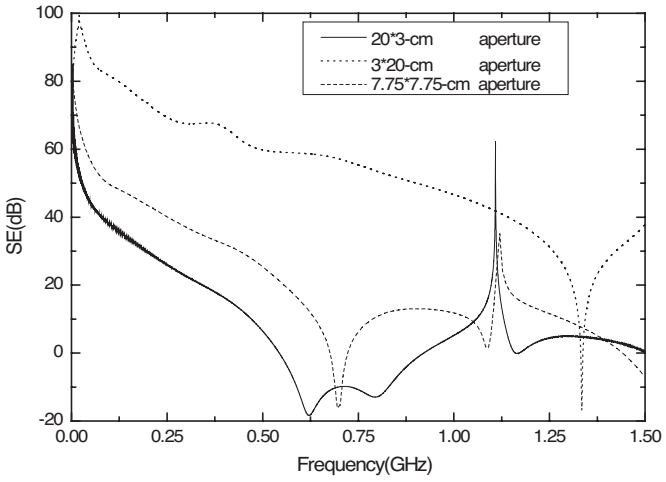

(a)

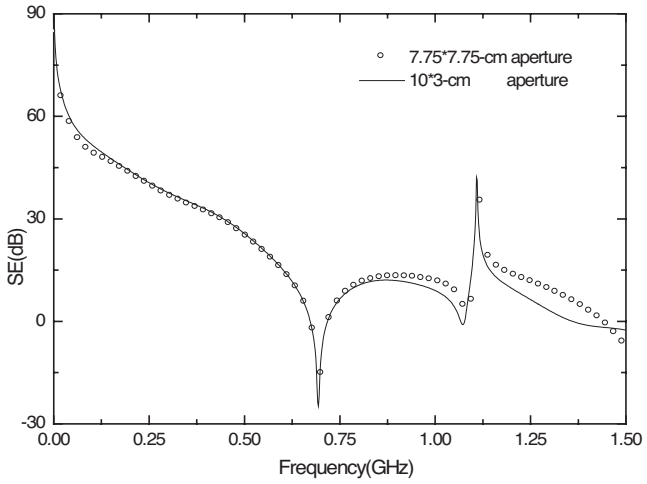

(b)

Figure 16. SE of different aspect ratio. (a) SE of different aspect ratio (b) the similar SE of different area.

4.3. Rectangular Apertures with Different Aspect Ratio

Based on the analysis above, we know that SE of rectangular apertures is worse than that of square apertures. We proceed to examine the influence that the aspect ratio of the rectangular aperture has

on SE. Fig. 16(a) plots the SE of the cavity with a 20 × 3-cm rectangular aperture (Fig. 4(a)), a 3 × 20-cm rectangular aperture and a 7.75 × 7.75-cm rectangular aperture. We observe that the SE curves vary significantly with the aspect ratio. In total, the larger the aspect ratio is, the worse the SE is. In Fig. 16(b), a 10 × 3-cm rectangular and a 7.75 × 7.75-cm rectangular apertures are seen to have the same SE, but the area of the square aperture is two times larger than the rectangular aperture.

So we should use the rectangular aperture with the smaller aspect ratio as possible as we can in engineering design.

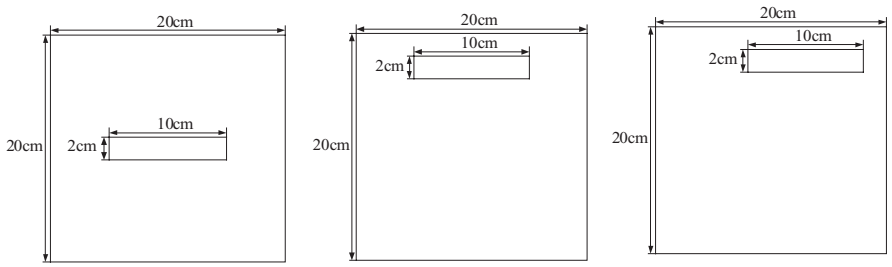

(a) Middle (b) Up (c) Oblique-up

Figure 17. The same aperture at different positions.

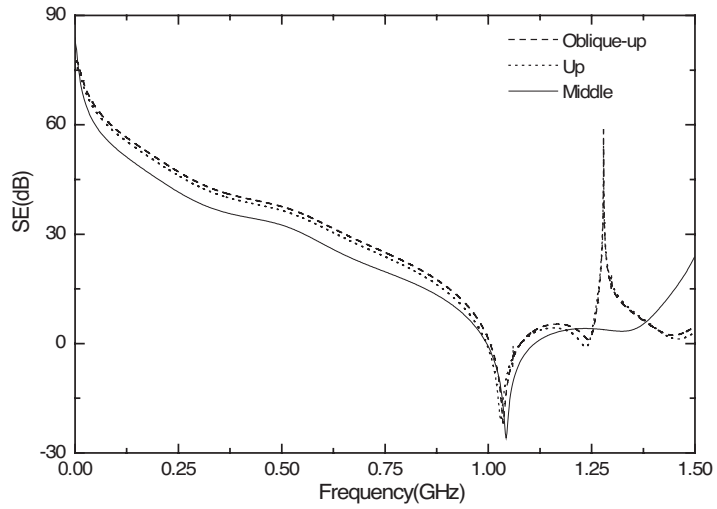

Figure 18. SE of the same aperture at different positions.

4.4. The Same Aperture at Different Positions

This section analyzes the SE of the $20 \times 30 \times 20$-cm cavity with the same aperture at different positions. As an example, a rectangular (10×2-cm) aperture is considered. Three cases are shown in Fig. 17. Fig. 18 plots the SE in three cases. In total, the SE of middle aperture (Fig. 17(a)) is the worst. The nearer the aperture is to the edge, the better The SE is. In addition, there is slight shifting of the aperture resonance at about 1050 MHz. For the up and oblique-up positions (Figs. 17(b) and (c)), the SE is very good up to 1.25 GHz, where the SE is about 60 dB.

Based on the results, electronic engineers should place apertures at the brim positions of the shielding box.

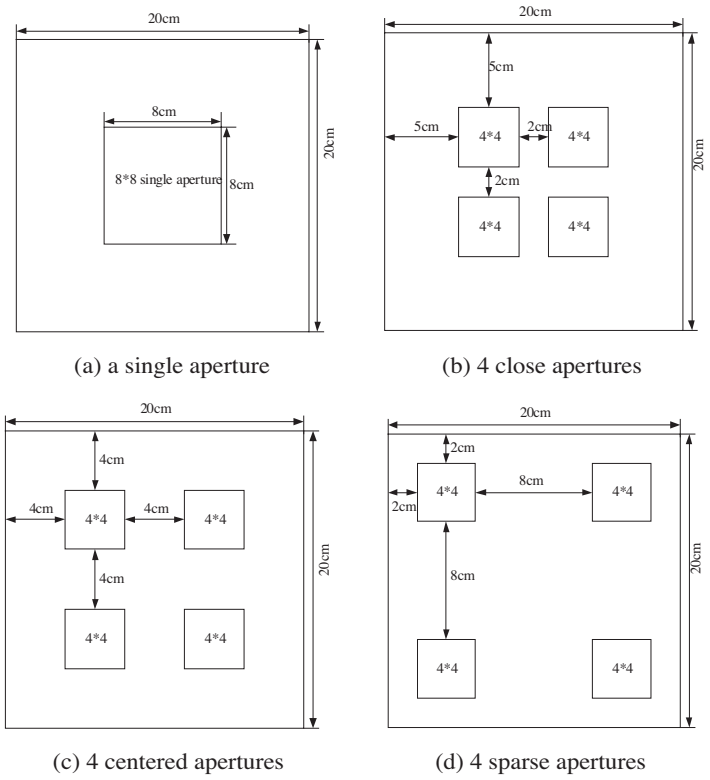

Figure 19. Apertures with different degree of closeness.

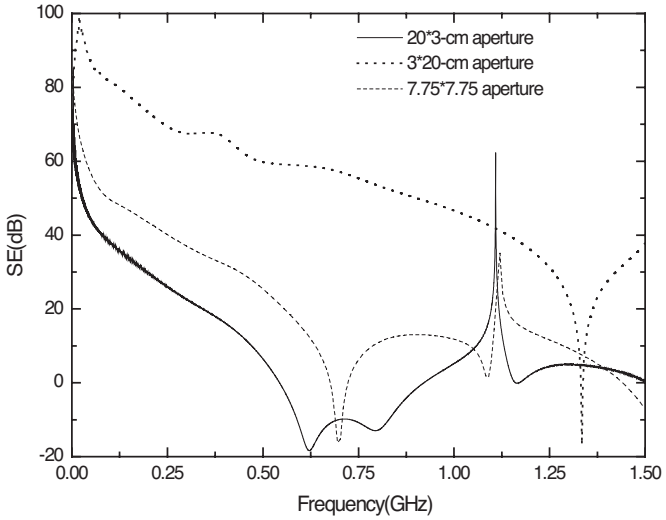

(a)

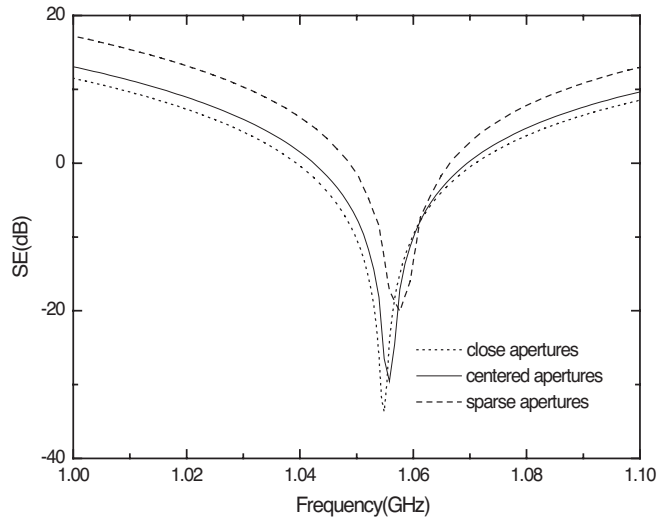

(b)

Figure 20. SE of apertures with different degree of closeness. (a) SE of four cases (b) partial enlarged drawing at resonance point.

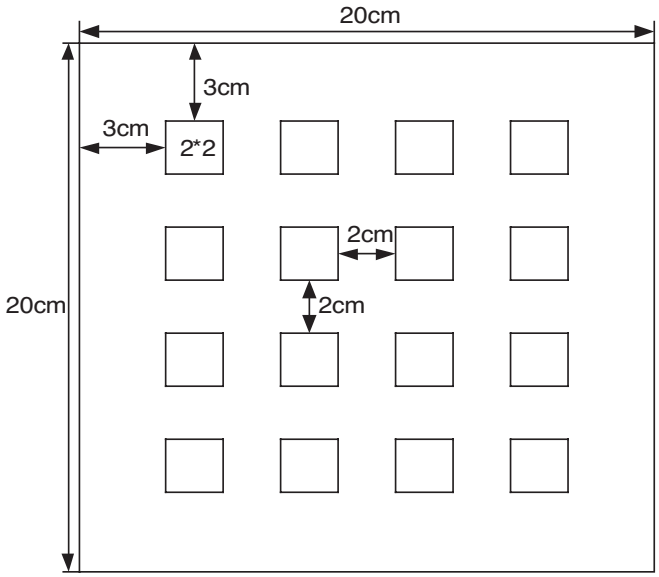

Figure 21. Sixteen apertures.

4.5. Degree of Closeness

Figure 19 illustrates the geometries of the 20 × 30 × 20-cm cavity with a single aperture and four small apertures with the same area with centered, close and sparse distribution. The SE of the four aperture configurations is shown in Fig. 20(a). Characteristically, all the geometries deteriorate the SE at low frequencies and better the SE at the high frequencies. Their resonant frequencies are different slightly (see Fig. 20(b)). Through comparing their curves, we find the SE of the cavity with the sparse aperture distribution is the best case. So in engineering, we should open sparse apertures.

4.6. Number of Apertures

The SE of the $20 \times 30 \times 20$-cm cavity with a single aperture (Fig. 19(a)), four apertures (Fig. 19(c)) and sixteen apertures (Fig. 21) is computed respectively. They have the same area. Their SE curves are given in Fig. 22. From 0 Hz to 1.50 GHz, the SE of all the structures falls and rises up in the following. The more the number of apertures is, the better SE is. In the practical engineering, opening a single large aperture should be avoided and some small apertures should be opened to improve the SE.

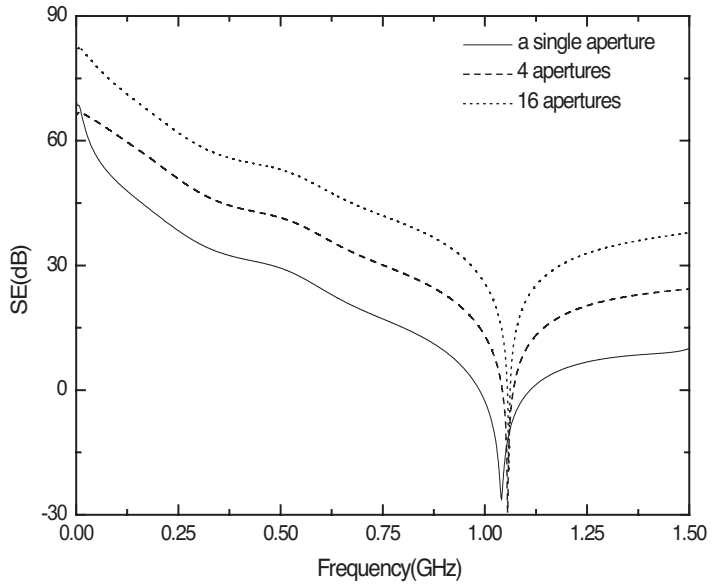

Figure 22. SE of different number of apertures.

5. CONCLUSION

Parallel FDTD method can only reduce the simulating time with the same time steps. Windowing can truncate the time-domain data to reduce the time steps. A novel hybrid method combining 3D Parallel Finite-Difference Time-Domain (FDTD) method with Windowing technique is proposed. The optimum virtual topology of Parallel FDTD for the scattering problem is also obtained. Besides, the Controlling factor, a key issue of the novel method, is discussed in detail. Combining Parallel FDTD with Windowing technique can enhance the computation efficiency greatly. Through computing some configurations by using the hybrid method, the paper obtains some useful conclusions.

REFERENCES

1. Mendez, H. A., "Shielding theory of enclosures with apertures," *IEEE Trans. on EMC*, Vol. 20, No. 3, 296–305, 1978.
2. Hill, D. A., et al., "Aperture excitation of electrically large, lossy cavities," *IEEE Trans. on EMC*, Vol. 36, No. 3, 169–177, 1994.

3. Robinson, M. P., et al., "Analytical formulation for the shielding effectiveness of enclosures with apertures," *IEEE Trans. on EMC*, Vol. 40, No. 3, 240–248, 1998.
4. Chen, H. Y., et al., "NEMP fields inside a metallic enclosure with an aperture in one wall," *IEEE Trans. on EMC*, Vol. 37, No. 3, 99–105, 1995.
5. Ma, S. and Y. Gao, "Analysis of enclosure with an aperture using FDTD method," *3rd International Symposium on EMC*, 242–245, 2002.
6. Zhang, Y., W. Ding, and C. H. Liang, "Study on the optimum virtual topology for MPI based parallel conformal FDTD algorithm on PC clusters," *J. of Electromagn. Waves and Appl.*, Vol. 19, No. 13, 1817–1831, 2005.
7. Georgakopoulos, S. V., et al., "HIRF penetration through apertures: FDTD versus measurements," *IEEE Trans. on EMC*, Vol. 43, No. 3, 282–294, 2001.
8. Siah, E. S., K. Sertel, and J. L. Volakis, "Coupling studies and shielding techniques for electromagnetic penetration through apertures on complex cavities and vehicular platforms," *IEEE Trans. on EMC*, Vol. 45, No. 2, 245–256, 2003.